THE JOURNAL OF PHYSICAL CHEMISTRY A

 VOLUME 105, NUMBER 30, AUGUST 2, 2001

ARTICLES

Collisional Properties of the OH Molecule

Anthony J. McCaffery* and Richard J. Marsh

School of Chemistry, Physics and Environmental Sciences, University of Sussex, Brighton BN19QJ, U.K.

Received: November 30, 2000; In Final Form: May 17, 2001

The disposition of the rovibrational levels in a diatomic molecule has a major influence on the outcome of inelastic collisions involving that molecule. In the case of the hydrides of moderately heavy elements, unusual collisional properties are anticipated in view of conflict between the demands of momentum and energy in these species. This arises because hydride rotational and vibrational quanta are generally large yet the species may be quite heavy and thus carry substantial momentum. This leads to competition between the momentum based *mechanism* for inelastic transfer and constraints which result from energy conservation. We illustrate these principles in investigating rotational, vibration−rotation, and quasiresonant vibration−rotation transfer, as well as vibrational predissociation of OH-containing van der Waals molecules. Collisional transfer is (almost) invariably constrained by energy conservation in this species and the impact of this on the linear-to-angular momentum mechanism is strongly evident in the collisional behavior of the OH molecule. Molecular collision partners may accept vibrational energy from OH without generating angular momentum, resulting in more efficient deactivation of vibrationally excited OH. Recent observation of emission from very high N levels of $(X)^2\Pi$OH in the nightglow appears to represent only the second recorded example of quasiresonant vibration−rotation transfer.

Introduction

It would be very beneficial to possess a rule-of-thumb guide to the state-to-state collisional properties of gas-phase molecules, an objective not as distant as it might have seemed a few years ago. The molecules of Earth's atmosphere form an important category for which greater insight would be valuable. This applies equally to the major components and to those minor constituents whose presence, even in minute concentrations, affects the properties of key regions. The OH radical is an example of this latter category. It is implicated in the chemistry of the troposphere, the stratosphere, and the mesosphere. It is also present in interstellar space. The $(X)^2\Pi \rightarrow (A)^2\Sigma^+$ transition is widely used to probe the spatial distribution of OH in flames, to measure quantum state distributions in the products of chemical reactions, to investigate the dynamics of van der Waals molecules, and in monitoring stratospheric OH levels. In each of these circumstances, detailed knowledge of the collisional behavior of OH would be advantageous, but the reality is that the picture is incomplete with experimental and theoretical data only patchily available. Little insight is given into factors *inherent in the OH molecule* which would guide us in interpreting the numerous collisional processes the species might undergo.

Here we give an overview of state-to-state collision dynamics of the OH radical using the angular momentum[1] (AM) theory of collisional transfer in which a common set of physical principles is applied to a wide range of inelastic processes (note that we do not include *electron spin* change at this stage). In this approach, the key factors that influence a molecule's collisional behavior are (i) bond length, (ii) rotational and

10.1021/jp004351b CCC: $20.00
Published on Web 07/11/2001

vibrational level structure within the molecule, and (iii) reduced mass of the collision pair. To emphasize this molecule-dependent commonality, we consider a number of aspects of the collisional behavior of OH, namely, rotational transfer (RT), vibration−rotation transfer (VRT), van der Waals molecule dissociation and quasi-resonant vibration rotation transfer (QRT). Each process is distinct, being characterized, for example, by different probabilities (cross sections or rate constants) and by different distributions among the final rotational states. OH emerges as an idiosyncratic species in its collisional behavior, principally because its rotational and vibrational separations are much greater than those of a homonuclear molecule of the same mass.

Background

We have demonstrated that collision induced processes in molecules may be understood using a transparent form of physics based on the angular momentum[1] theory of rotational transfer in which the primary *mechanism* constitutes linear-to-angular momentum (LM → AM) interconversion constrained to operate within *boundaries* set by energy conservation. We find that the LM → AM mechanism appears to be a constant feature in collision-driven events including RT, VRT, and QRT, as well as in chemical reactions. The boundary conditions on the other hand vary very widely indeed and it is the variation in the energy conservation conditions that gives the rich diversity of behavior seen in these different processes.

The angular momentum (AM) model was proposed initially in the context of pure RT.[1] A rotational *transfer function* was formulated[2] based on LM → AM interconversion via a torque arm or effective impact parameter (b_n), shown from analysis of experimental data[2] to be of molecular dimension. For a homonuclear diatomic, the maximum value of this quantity, b_n^{max}, is often half the bond length (HBL) though for a heteronuclear species, the identification of b_n^{max} is somewhat more complex as we describe below. Quantitative calculations using a hard ellipsoid representation of the potential and Monte Carlo simulation of collision trajectories agree well with experiment.[3] In a number of instances, the maximum value of b_n in a homonuclear species is constrained to be less than HBL. This is the case in pure RT when initial rotational state $N_i \gg 0$ and/or when collision partner mass is high.[4] In the case of RT, the shape of the distribution function in ΔN typically is unchanged (though the overall probability is reduced),[4] remaining exponential-like in all cases. In VRT restrictions on b_n can dramatically alter the shape of the rotational distribution. The circumstances under which this occurs are discussed below.

Vibrationally inelastic processes are readily incorporated into the AM model. Initial calculations[5] involved vector subtraction of the appropriate amount of linear momentum to open the vibrational channel from each trajectory with that remaining available for conversion to rotational AM. This approach was found to successfully explain VRT in CO_2−H* collisions using the hard-ellipse, Monte Carlo method.[5,6] More recently, we have utilized a model in which the vibrational "barrier" constitutes no more than an energy constraint on individual rotational channels as represented in velocity−AM diagrams. This method, despite its simplicity, reproduces experimental VRT data quantitatively.[7] This new boundary condition, found in VRT but absent in RT, causes a marked truncation of the low ΔN region of the rotational distribution.[8] When the vibrational barrier is large, this effect is sufficiently marked that the resultant shape may superficially resemble a Boltzmann distribution. It is however an exponential-like function in which low ΔN probabilities have been reduced to a greater or lesser degree depending on the magnitude of the vibrational barrier.

VRT from highly excited diatomics may lead to quasiresonant vibration rotation transfer (QRT), a collision-induced process which occurs only under conditions of quasiresonance in energy *and* in AM.[9] This leads to very sharply peaked rotational distributions which have been observed thus far only in Li_2.[10] Theoretical calculations indicate that QRT is likely to be a feature of the collisional properties of diatomic hydrides,[9,11] and the action of chemical lasers is thought to be enhanced by processes similar in kind to QRT.[12] This peaked distribution also represents an exponential-like fall but in this case, very sharply defined energy conservation boundaries severely limit the range of b_n values for all inelastic channels except the quasiresonant state.[13] The conditions which give rise to QRT are primarily a function of the disposition of the molecule's energy levels.

Each of these processes, namely RT, VRT and QRT may occur in the OH molecule and here we investigate these in some detail. As mentioned above, we find that the OH molecule is unusual in many respects and this stems from the asymmetry of the mass distribution and its effects on both the bond length and the energies of the quantum states of this species. The findings reported here are of relevance to other heteronuclear hydrides, the halides, for example. We make predictions of likely collisional distributions in RT, VRT and QRT and where possible relate these to experimental determinations. In some instances, no experimental data is available. For the most part our predictions are based on the simple physical arguments that form the basis of the AM theory[1] and make extensive use of velocity−AM diagrams[14] in so doing. *This is done to meet the objective set in the opening sentence of this work*. We have demonstrated[4,5,7,9] that RT, VRT and QRT may be predicted quantitatively using hard ellipsoid Monte Carlo calculations based on LM → AM interconversion.

In its most concise form, the mechanism of LM → AM interconversion may be written as

$$\Delta N = \mu v_{rel} b_n \tag{1}$$

where ΔN is the change in rotational AM, μ the reduced mass of the collision partners, v_{rel} is the velocity of relative motion, and b_n the effective impact parameter or torque arm. Equation 1 will be referred to in what follows as the A-equation. The boundary conditions imposed by energy conservation is expressed as follows for processes involving vibrational state change:

$$\Delta N = \sqrt{(N_i + {}^1/_2)^2 - (\omega\hbar\Delta\nu \pm \mu v_r^2/2)/B} - (N_i + {}^1/_2) \tag{2}$$

Here B is the molecule's rotational constant and $\omega\hbar\Delta\nu$ is the energy associated with the vibrational transition. In what follows, this will be referred to as the E-equation. A further equation, given in a number of earlier papers,[5] expresses combined energy and AM conservation and is referred to as the (E+A) relation.

A transfer function for RT based on the A-equation was derived by Osborne and McCaffery[2], an approach which assumes the separability of probability densities of AM change and of energy change. We have suggested[8] that *rotational distributions in all forms of collisional transfer are derived from that predicted by the transfer function. The (sometimes very dramatic) deviations from this "natural" distribution are the result of changes in the energy boundary conditions*. This principle will be amplified in the context of the OH molecule in this work. We give the transfer function below since it

illustrates the central role played by the quantity b_n in the following model:

$$P(N_f|\, N_i)dj_f = C\int_0^{b_n^{max}} P(l|\, b_n)P(b_n)b_n db_n dN_f \delta(|E_{tot} - E'_{tot}|)\delta(|\, J_i - J_f|) \quad (3)$$

The components of this equation are discussed in ref 1 and in a number of recent papers. Here we do no more than draw attention to the importance of the *range* of b_n in determining the overall probability of RT and embodied in the value b_n^{max}. Note that eq 3 predicts an inverse power dependence on ΔN, as observed experimentally when the available data is extensive.[15] In many collision systems, the data do not allow unambiguous identification of the functional form and we use the expression "exponential-like" to describe the natural form of pure RT.

Besley et al.[14] demonstrated that both A- and E-equations are readily represented in plots of relative velocity against *change* in rotational AM. Threshold or channel-opening velocities are calculated from eqs 1 and 2 (using b_n^{max} = HBL in eq 1) and illustrate very graphically the influence of the boundary conditions on the mechanism. The plots are collision system-specific and vary widely as molecule and collision partner change. This form of representation also allows the velocity distribution to be shown and thus all kinematic elements are present. In recent papers[4,8] we have shown that a limited number of patterns of A- and E-equation plots appears to exist and that much collisional behavior can be related to one or more of these generic forms. Thus, for example, the distinctive E-plot found on analysis of QRT in Li_2[13] may be used as a signature of a related process in HF[9] and in the highly excited or "superrotor" states of Li_2.[16,17]

OH Molecule

As a result of the development of LIF as a convenient means of detecting OH, spectroscopic parameters of both ground $X^2\Pi$ and excited $A^2\Sigma^+$ states are well-known. Quantitative LIF detection is impeded by population loss through inelastic transfer and knowledge of collisional properties are important in this context. Studies of RT and VRT of this molecule in its excited state have been performed by Crosley and co-workers[18,19] and by Jörg et al.[20] among others. The choice of collision partner has frequently involved other atmospheric constituents, such as N_2 and O_2, although Ar and He, as well as H_2 and other species, have also been used. Emission from high lying rotational levels of the $X^2\Pi$ state has been observed in the night airglow[21] and in rocket-borne experiments[22] and there are strong indications of non-Boltzmann distributions. These observations are significant in atmospheric modeling in view of the widespread assumption of a local thermodynamic equilibrium among species.

Much interest has centered on the weakly bound complexes that OH forms when cooled in a supersonic jet and the high quality photodissociation experiments carried out on OH−Ar by Lester and co-workers[23] have relevance to the topics discussed here, particularly those in which the ejection of an Ar atom follows excitation of one quantum of OH vibration. This can be viewed as a process in which the $v = 1$ vibrational momentum of OH is imparted to an (almost) stationary Ar atom and recoils into rotational levels of $v = 0$ in the process. This latter event is readily analyzed in the same way as the more usual form of collision in which there is momentum of relative motion.

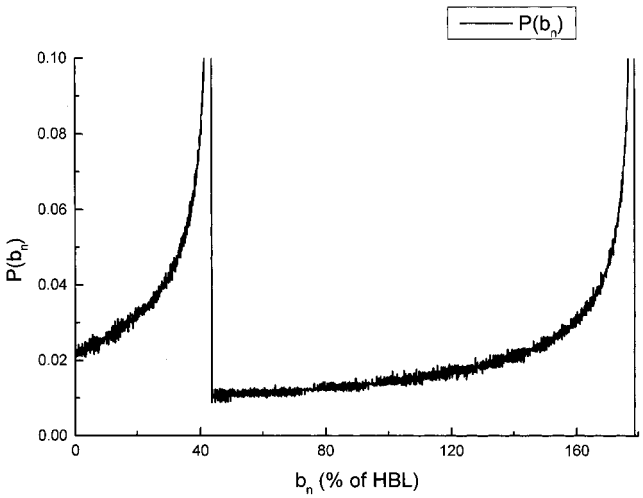

Figure 1. Probability density of effective impact parameter $P(b_n)$ for an acentric ellipse representing the repulsive wall of a heteronuclear diatomic molecule. This is obtained through a Monte Carlo method in which b_n is calculated for each of 2×10^6 trajectories and counted in 0.1% bins. For OH, this yields values $b_n^{max} = 0.88$ and 0.13 Å for the H and the O ends, respectively. Note that, for a homonuclear diatomic, a single peak at half bond length would be obtained.

In the analysis of collision-induced transfer described here, our emphasis centers on the *kinematic* properties of the collision pair and the distribution of nuclear mass in OH is central to this. OH has its center-of-mass (CM) very close to the center of the O-atom and a reasonable description of the repulsive wall of the potential might be egg-shaped with the O-atom at the big-end. A representation in the form of an acentric ellipse is also possible.[24] Of particular relevance here is the possibility that the molecule possesses *two* torque arms, one extending from the CM to the O atom and the other to the H atom. The division of these (the sum should in general be close to the bond length) depends somewhat on our choice of representation of the hard shape to be elliptical or egg-shaped. Once this decision is made then the numerical value is readily obtained in a Monte Carlo trajectory calculation from which the function $P(b_n)$ is extracted. For a heteronuclear species this is a double valued function which, for elliptical OH, is shown in Figure 1. to peak at 0.88 and 0.13 Å. In a similar calculation on a homonuclear diatomic $P(b_n)$ is found to be single valued with peak at half bond length (HBL).

In view of the large difference between torque-arm lengths of the *H* and the *O* end of the molecule, one might anticipate that most RT for example would occur as a result of collisions with the H end. As we see below, for the majority of collision partners, kinematic factors prevent the use of the full b_n^{max} given above. In what follows we analyze RT, VRT, and QRT in the OH molecule using the AM model as represented by eq 1 modified by the boundary conditions that eq 2 embodies. The LM → AM *probability* is given by eq 3. The effect of energy constraints is often to make this relationship rather opaque although it is intuitively clear that a reduction in the range of b_n is likely to reduce the overall probability. Most of our deductions will be made from the graphical representations of eqs 1 and 2 in the form of $v_{rel}-\Delta N$ plots in order to reveal the physical processes at work. As stated earlier, we have demonstrated the capability of hard ellipsoid-Monte Carlo calculations based on this model to reproduce experimental data quantitatively.

Rotationally Inelastic Transfer

5.1. Excitation. We have illustrated the complex kinematic factors that determine the efficiency of pure RT in atom−diatom collisions[4] using $v_{rel}-\Delta N$ diagrams to display the physical principles in operation and multihard ellipsoid Monte Carlo calculations for quantitative confirmation. Collision reduced mass and initial rotational state both play a significant role, the former because as μ increases, greater momentum is carried for a given velocity and this hastens the onset of an energy constraint. The latter is the result of changes in energy gap associated with unit change in rotational quantum number as N_i increases.

That unusual collisional properties might be the norm in molecules such as OH was alluded to earlier. The acentric mass distribution and short torque-arm mean that collisional behavior will be very different to that of, for example, Li_2, which has similar molecular weight. This is seen clearly in plots of the A (eq 1) and E (eq 2) relations for OH−Ar collisions shown in Figure 2a. Figure 2a is plotted for $N_i = 0$ and in many diatomics undergoing RT from the lowest level, the system would be *AM-constrained*, i.e., the A-plot would lie to higher velocities of the E-plot for all ΔN and thus permit all b_n values up to the limit imposed by the molecule's dimensions. OH however has a rotational constant that is large for its mass and so the system is in fact strongly *energy* constrained for all ΔN. A dominant energy constraint (as in this case for OH−Ar) is known to inhibit RT.[4] The LM → AM mechanism is required to operate strictly within conditions of energy conservation and in order for these to be met, the range of values that b_n in eq 3 may adopt becomes restricted[4,5,14] to a degree dependent on the magnitude of the energy constraint. This effect is very marked in Li_2, Na_2, and other species as initial rotor state increases.[4] Dominance of AM constraint on the other hand is an optimal kinematic condition for RT since the maximum value that b_n may take is restricted only by the maximum anisotropy of the molecule concerned.

The energy constraint represented in Figure 2a is very severe. For $v_{rel} = 600$ m s^{-1} the A-plot indicates that the $\Delta N = 10$ channel is open via the LM → AM mechanism (drawn in Figure 2a for $b_n^{max} = 0.88$ Å) but energy conservation limits opening of channels beyond $\Delta N = 2$. This apparent conflict between the E- and A-relationships is resolved by calculating that maximum value of b_n which permits simultaneous energy and AM conservation[4,5] through the E+A equation mentioned earlier. In general, this must be done for each ΔN channel (though the solution for just one channel is needed when $N_i = 0$), and a modified A-relationship is plotted. This is shown in Figure 2a as the modified A-plot for OH−Ar. As discussed in ref 4, restrictions on range in b_n is a strong function of collision partner mass. The maximum value of b_n is 0.19 Å for Ar, 0.21 Å for N_2 and 0.49 Å for He as collision partners of OH in $N_i = 0$. The H atom as a collision partner is sufficiently light that no reduction of b_n is required to meet energy conservation.

Note that despite these energy enforced constraints on b_n, the collision-induced ΔN_f state distribution is expected to be exponential-like [4] since the $\Delta N = 0$ channel is open for all values of v_{rel} whatever the b_n value. The form of the $P(b_n)$ function in the rotational transfer function is such that low ΔN are strongly favored over high. Figure 2a shows (arrow) the most probable relative velocity for a Maxwell−Boltzmann distribution of OH−Ar at 300 K. This is barely sufficient to meet the channel opening condition for $\Delta N = 3$ and it is clear from the plot that rate constants or cross sections for collision-induced processes above $\Delta N = 6$ will be very small.

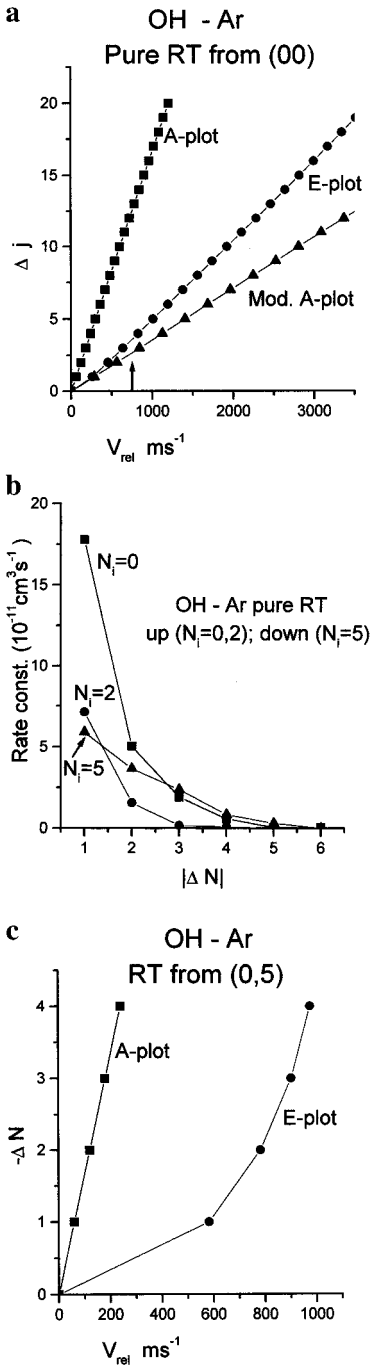

Figure 2. (a) Plot of A-relation (eq 1) and E-relation (eq 2) for rotational excitation from the (0, 0) level in $(A)^2\Sigma^+$OH−Ar collisions. The plots indicate that the LM → AM mechanism is constrained by energy conservation and must be modified. This is achieved by limiting the maximum value b_n may take in eq 1. The appropriately modified A-plot is also shown. The arrow indicates the most probable relative velocity for this collision pair at 300 K from which it can be seen that RT beyond $\Delta N = 6$ will be of low probability. (b) Plots of RT in OH−Ar collisions. Filled squares represent RT from $N_i = 0$ circles show data fom $N_i = 2$. Data obtained from Degli Esposti and Werner (ref 25). The triangle points plot rotational relaxation from $N_i = 5$ using data from ref 20. Note that fine structure components are summed in the results shown. (c) A- and E-plots for rotational relaxation from (0, 5) in $(A)^2\Sigma^+$OH−Ar collisions. Constraints on low ΔN are much more stringent than for rotational excitation (Figure 2a)

Comparison with experiment is not straightforward as the early determinations of RT rates using N_2, Ar, and H_2 by Lengyel and Crosley[18] were felt to be less than wholly reliable by later workers.[20] Jörg et al.[19] have measured rate constants

for *downward* transitions from $N_i = 5$. Below, we show this to be a quite different case to rotational excitation. The results of Jörg et al. are in good agreement with the quantum scattering calculations of Degli Esposti and Werner[25] who have also calculated rate constants for upward transitions from low N_i and comparison is best made with these data. The calculated rate constants show the very limited series of ΔN states accessible at 300 K and the rapid drop in magnitude of rate constants as N_i increases is very clear. They fall in exponential-like fashion with ΔN as shown in Figure 2b which displays OH−Ar data of Degli Esposti and Werner for $N_i = 0, 2$. Note that in these plots we have summed contributions from F_1 and F_2 fine structure components to a particular N_f.

5.2. Relaxation. Figure 2c shows A- and E-plots for $5 \rightarrow -\Delta N$ for OH−Ar collisions. The LM → AM mechanism is *much* more strongly energy constrained at low ΔN than for $(0 \rightarrow +\Delta N)$. Curvature in the E-plots results from the diminishing energy gap between successive N levels as ΔN increases. Because of this curvature, restrictions in the range of b_n values accessible will be *channel-dependent* with low ΔN channels suffering the greatest restriction.[4] Calculated maximum values for b_n in OH−Ar for transitions from $N_i = 5$ are 0.088, 0.121, 0.144, and 0.167 Å for $\Delta N = -1, -2, -3$, and -4, respectively. This is sufficient information to predict the overall shape of the rotational distribution. An exponential-like form is anticipated since $v_{rel} = 0$ for $\Delta j = 0$ for both E- and A-relations but low ΔN processes will be diminished in comparison to the case shown in Figure 2a. However, the high ΔN end of the distribution is expected to be enhanced by comparison to the case of rotational excitation from $N_i = 0$ and thus a shallower, flatter curve is expected. In Figure 2b we plot the experimental RT data of Jörg et al. for OH−Ar and the change in shape compared to the process $N_i = 0, 2 \rightarrow + \Delta j$ (also plotted) is very apparent.

The above analysis has been purposefully qualitative to demonstrate how the transparent physics of the AM model allows rule-of-thumb predictions of RT distributions in differing circumstances. The reduction of rate constant with increasing N_i, observed in many systems, has, in the past,[26] been interpreted in terms of the averaging of the anisotropy said to take place as the rotor speed approaches the "duration time" of the collision. This approach leads to the introduction of new parameters as well as the ill-defined concept of "duration" of the effective interaction and appears unnecessary. Kinematic factors alone are sufficient to account for the variation in rate constants and cross sections as initial rotor state increases.[4] Following a survey of theoretical methods, Korsch and Ernesti concluded, that "*amazingly simple models allow very precise description of experimental RT results*".[27] Hard ellipsoid Monte Carlo calculations based on LM → AM reproduce RT data quantitatively.[3] The value of a preliminary analysis using the v_{rel}−AM diagrams is that the factors that govern the outcome of collisional phenomena are readily identified. These turn out to be quantities as prosaic (and as readily available) as the energies of the rotational (and for VRT the vibrational) states of the molecule concerned as well as bond length, atomic size and relative velocity. Little of the detail of the intermolecular potential enters into this analysis.

Vibration−Rotation Inelastic Transfer

The study of vibrational transfer in molecules has a long history[28] involving many different experimental techniques. Much of the early development took place separately from the study of RT and relatively few experiments on vibrational transfer include a complete determination of final rotational populations. We have pointed out[8] that there appears to be little consistency in the determination of vibrational transfer rate constants which are often ill defined in terms of initial and final rotational states. Williams and Crosley report rotationally resolved rate coefficients for $OH(A)^2\Sigma^+(1, 2) \rightarrow (0, N)$ using a wide range of collision partners. This process constitutes vibrational *relaxation* together with rotational excitation and, as in the case of pure RT discussed above has inherently different characteristics to vibrational and rotational excitation. We therefore first briefly discuss what might be expected in a VRT *excitation* collision from $v = 0$ before analyzing the experimental data of Williams and Crosley.

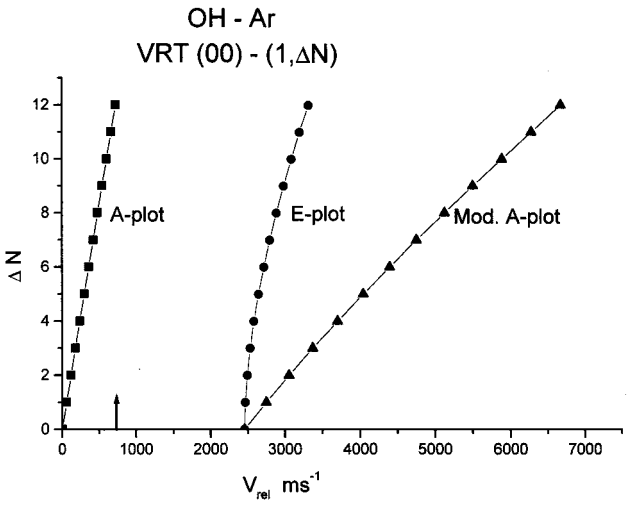

Figure 3. A-, E-, and modified A-plots for vibration−rotation excitation from (0, 0) in $(A)^2\Sigma^+OH-Ar$ collisions. At least 2450 m s^{-1} of relative velocity is needed to open (1, ΔN) channels. Little of a 300 K Maxwell−Boltzmann distribution (arrow represents most probable velocity) would achieve this value.

6.1. Vibrational and Rotational Excitation. Rotational distributions resulting from VRT excitation were analyzed recently in the diatomics Li_2, NO, and HF.[8] In this series, the vibrational gap increases, with Li_2 having lowest and HF highest requirement. The effect of this on the distribution of rotational levels is very dramatic since it causes a shift of the peak away from $\Delta N = 0$ found in pure RT, to some higher value dependent mainly on the magnitude of the momentum gap[8] relative to the rotational separations. The origin of this effect may be seen in the velocity−AM plot for the OH molecule in collision with N_2 shown in Figure 3. The unmodified A-plot drawn using eq 1 implies that rotational AM may be generated without opening the vibrational channel. The E-plot however demonstrates that there is a barrier equivalent to 2600 m s^{-1} of $(OH-N_2)$ relative velocity to be overcome *before* AM may be generated in the $v = 1$ vibrational level.

This is readily treated within the AM model. The unmodified A-plot assumes b_n is unrestricted and can take any value up to that (b_n^{max}) available from the repulsive anisotropy. In OH, the value of 0.88 Å is appropriate. Under conditions of energy constraint, however, this maximum value may not be attainable[4,5] and a new upper limit to b_n is calculated to be consistent with simultaneous energy and AM conservation. In the kinematic circumstances illustrated in Figure 3, very drastic reductions in this parameter are required for low ΔN transitions and this leads to much reduced VRT probabilities particularly in the low ΔN region.

Thus, rather than the exponential-like fall of rotational populations, the 'natural' form found in pure RT, VRT is

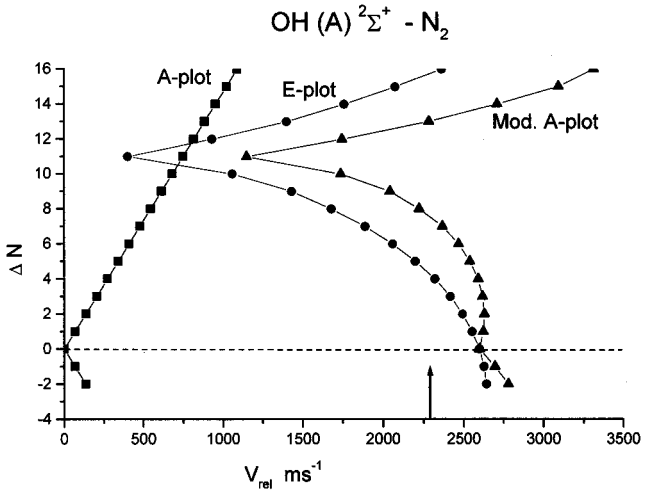

Figure 4. As for Figure 3 but representing vibrational relaxation from the (1, 2) state of OH. The distinctive shape of E- and modified A-plots are responsible for the "bimodal" appearance of experimental rate constants involving this process in OH. The arrow indicates the relative velocity that would be required to excite the $0 \rightarrow 1$ vibration in N_2

characterized by a distribution that is a truncated exponential with reductions in the low ΔN region. The maximum probability shifts from $\Delta N = 0$ and in some circumstances, this leads the distribution to be reminiscent of the Boltzmann distribution, a similarity that has led authors to fit experimental data to an assumed Boltzmann form and to extract a rotational "temperature". The shift in the peak of the VRT distribution is found[8] to increase as the vibrational momentum gap increases and thus quoted rotational "temperatures" may in reality provide little more than a measure of the characteristic vibrational energy of the molecule undergoing inelastic transfer.

This potential misidentification of rotational populations in VRT has implications for atmospheric studies where the assumption of a local thermodynamic equilibrium is frequently made even in regions where this appears an unlikely possibility. We return to this topic below following discussion of the QRT mechanism in highly excited OH. Figure 3 shows the modified A-plot which now operates within energy conservation conditions for all ΔN. Also shown is an arrow representing the most probable relative velocity for OH−N_2 collisions. This is well short of the $v = 1$ channel-opening velocity and it is clear that only a minute portion of molecules from the Maxwell−Boltzmann distribution have velocity sufficient to contribute to VRT from $v = 0$ and as a result, these processes will have low probability under normal laboratory conditions. However, in the upper atmosphere, the presence of vibrationally excited N_2 or O_2 molecules would markedly change this situation as would translationally hot atoms produced by photodissociation.

6.2. Vibrational Relaxation, Rotational Excitation. Williams and Crosley[19] report rate constants for the process OH-$(A)^2\Sigma^+(1, 2) \rightarrow (0, \Delta N)$ induced by collisions with Ar, N_2, and O_2. This constitutes an unusual kinematic situation since the transitions represent an energy reduction at the same time as rotational AM increases. This is the case up to $\Delta N = 11$ from which point the energy gap begins to increase as ΔN rises. The appropriate velocity−AM diagram for N_2 as a collision partner is shown in Figure 4. The structure of this plot reflects the pattern of the molecule's quantum states and changes relatively little with collision partner. It reveals a very different picture to the processes of pure RT (Figure 2a) or of vibrational and rotational excitation (Figure 3). Experiment indicates that there are significant differences in the efficiency of VRT when N_2 is

TABLE 1: Maximum Values of b_n for Individual ΔN Channels for VRT in OH−N_2 Collisions

ΔN	b_n^{max}/Å	ΔN	b_n^{max}/Å
0	0	8	0.215
1	0.023	9	0.264
2	0.045	10	0.345
3	0.068	11	0.575
4	0.093	12	0.413
5	0.118	13	0.341
6	0.146	14	0.310
7	0.177	15	0.291

collision partner compared, for example, to Ar (cross sections are 30.1 and 0.56 Å for N_2 and Ar, respectively), and these differences may be examined using the $v_{rel}-\Delta N$plots.

Velocity−AM plots similar to Figure 4 are observed in other vibrational relaxation processes.[8] In OH an energy near-resonance is found at $\Delta N = 11$, too large an AM gap to produce the sharply peaked distributions that are the feature of quasiresonant vibration rotation transfer.[9,13] An unusual feature of this VRT process is that momentum and energy for the generation of rotational excitation is taken from the OH molecule itself and is available only as that of a single vibrational quantum, equivalent to 2599 m s^{-1} of relative velocity for OH−N_2. Table 1 lists the new maximum values of b_n permitted within energy conservation for each channel. These are useful in obtaining a rule-of-thumb guide to the ΔN distributions following collision. It is of interest to note that for $\Delta N > 7$ (of those listed in Table 1) the maximum value that b_n may take is greater than for pure RT in these same systems (where energy constraints restrict b_n to be no more than 0.21 Å for all ΔN). This unusual situation can be expected to have an influence on the overall shape of the ΔN distributions.

We first consider the change in relative VRT probabilities in OH on changing collision partner from Ar to N_2. As mentioned above, the cross sections vary by a factor of around 50. We focus first on the case of OH−Ar the $v_{rel} - \Delta N$ plot for which is very similar to Figure 4. Before analyzing the kinematics of this encounter, we digress briefly to the subject of overall angular momentum conservation. The inelastic process described here shares certain similarites to a reactive collision as a result of the energy release as the vibrational mode of OH deactivates and raises questions as to how overall energy and AM are conserved.

Total angular momentum $\mathbf{J}$ ($= \mathbf{l}_i + \mathbf{N}_i$, where $\mathbf{l}_i$ is the initial orbital AM and $\mathbf{N}_i$ is the initial rotational AM) is conserved and so $\boldsymbol{J} = \boldsymbol{l}_f + \mathbf{N}_f$, where the subscript f refers now to postcollision quantities. Thus, $\mathbf{l}_i + \mathbf{N}_i = \boldsymbol{l}_f + \mathbf{N}_f$ or alternatively $\Delta\mathbf{N} = -\Delta\mathbf{l}$. For vibrational relaxation coupled with rotational excitation, energy and momentum released by OH when it undergoes vibrational deexcitation represents a greater contribution than that available from relative motion of the two species.

The mechanism of LM $\rightarrow$ AM interconversion is inefficient in most circumstances in the OH molecule for the reasons discussed in earlier sections. The orbital AM available in OH−Ar relative motion as a result of the $(v = 1) \rightarrow (v = 0)$ transition in OH is around $40\hbar$ which must be matched by the rotation induced in the diatomic in order to conserve total $\mathbf{J}$. However, the corresponding *energy* is equivalent to no more than 14 or so units of ΔN (Figure 4 showing OH−N_2 is a guide). There is a substantial mismatch therefore and as a result, outgoing trajectories are very strongly limited. Thus, energy and AM conservation together force the collisional process to be very much constrained in $b_n$values both in generating ΔN and in matching this in the exit trajectory to produce $-\Delta l$.

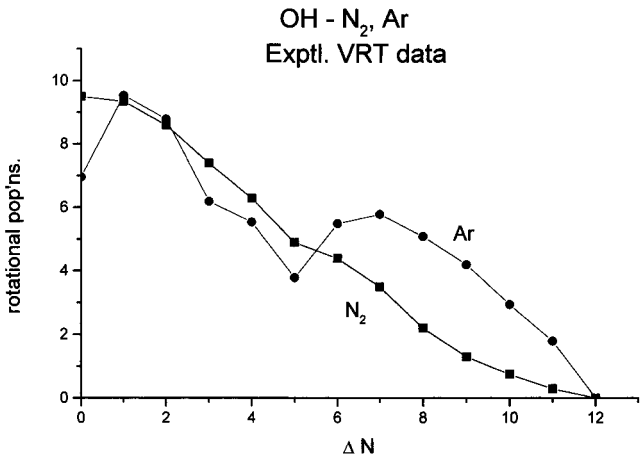

Figure 5. Experimental rate constants for VRT (1, 0) → (0, Δ*N*) for OH in collision with N_2 and Ar. Data replotted from Williams and Crossley (ref 19). The plots are normalized to represent both on the same graph. In reality, the OH−N_2 rate constants are 50 times greater than those obtained using Ar as collision partner.

The shape of the Δ*N* distribution reported by Williams and Crosley[19] is shown in Figure 5, though now plotted against Δ*N* rather than N_f as in the original. The maximum is dispaced to low Δ*N*, a characteristic of VRT processes arising from stringent restrictions of available b_n values as described above. New maximum values of b_n are listed in Table 1 and increase steadily from $\Delta N = 0$ up to 11 after which they begin to decrease. This is to be set in the context of the rapidly dropping probability of Δ*N* change as *magnitude* of Δ*N* increases and which is limited by available energy in this case to around 12.

The experimental curve peaks at low Δ*N* and then drops rapidly before recovering to yield a second peak at $\Delta N = 7$. The shape of the modified A-plot indicates that bimodality in this distribution is to be expected. The maximum value of b_n increases and contributing relative velocities become more probable as Δ*N* increases. If all Δ*N* values were equiprobable the distribution would peak at $\Delta N = 11$. They are not however and the exponential-like fall in this probability leads to a displacement of the second peak. However, the presence of this second peak can clearly be seen to arise from the effect of energy constraints on the mechanism and can be expected whenever this form of VRT takes place in OH. It is observed for OH−O_2 and OH−N_2 collisions, though only vestigially in the latter case because of the strength of the low Δ*N* processes.

The efficiency of combined vibrational relaxation and rotational excitation in OH−N_2 collisions illustrates the importance of the energy and AM conservation relationships discussed above. The v_{rel}−Δ*j* plots show an arrow on the velocity axis representing that velocity required to excite the (0 → 1) vibrational transition in N_2. The diagram makes clear that it is close in energy and velocity to that released by the OH molecule during the (1→ 0) process and thus it may act as a *sink* for the release of the troublesome vibrational energy emanating from the OH *source*. However, it is important to recognize that this is an energy sink having the special property that it *may absorb the vibrational energy but generates no angular momentum in the process*. For this collision system, some 36ℏ of orbital AM may be generated in the OH vibrational deactivation of which up to 32ℏ may be absorbed by vibrational excitation of N_2 and thus an AM mismatch of no more than four units exists when N_2 is the collision partner. This is readily accommodated using the velocity of relative motion of the two species.

The VRT pattern in OH−N_2 (Figure 5) closely resembles conventional 'upward' VRT (i.e., vibrational and rotational excitation)[8] though close examination reveals that it is similar in form to the small vibrational gap limit. This results from the convenient disposal of OH vibrational energy into the N_2 mode in the form of V−V transfer and thus the gap to be overcome by the OH−N_2 relative motion is equivalent to only around 300 m s^{-1}, well within the 300 K Maxwell−Boltzmann velocity distribution which peaks for this collision pair at 775 m s^{-1}. In these circumstances the second peak around $\Delta N = 6$ is likely to be less prominent but can be seen as a slight bulge on the side of the experimental distribution at $\Delta N = 6$ and 7.

6.3. Vibrational Predissociation of OH−Ar van der Waals Complex. The vibrational deexcitation of OH and associated rotational excitation induced by collisions with Ar, discussed above, has close similarities to the dissociation of the OH−Ar van der Waals (vdW) complex induced by exciting one quantum of the OH vibration. The wide-ranging experimental study by Lester and co-workers[23] has yielded a very detailed picture of quantum state distributions under different photodissociation conditions. This process could be considered as analogous to collision-induced VRT, but now the Ar atom is effectively stationary, the impulse stemming from the vibrational motion of the OH bond with little velocity of relative motion.

As in the case of VRT with this collision pair, there are problems of AM and energy conservation to be overcome in disposing of the vibrational excitation. AM generation is much restricted by energy constraints as discussed above. In the decomposition of a vdW complex, there is an energy cost to surmounting the barrier to form separate fragments. In the case of OH−Ar this constitutes a "reservoir" for absorbing some of the energy of deactivation of the OH bond. The well depth is calculated by Degli Esposti and Werner to be 1100 cm^{-1} [25] and following escape of the molecule, it is straightforward to show that some 950 m s^{-1} remain for disposal into rotation *and* the orbital AM required to meet AM conservation.

Figure 4 represents the kinematics of vibrational relaxation and rotational excitation originating on the OH(1, 2) level and changes relatively little when Ar is the collision partner. It may be used to analyze data from the experimental study of Berry et al.[23] of vibration-induced dissociation of OH−Ar from that level. 950 m s^{-1} will open channels up to around $\Delta N = 10$ if all of this is used in rotation. However, AM conservation requires that the orbital AM of recoil match that of the rotor, the velocity for *both* of these coming from the residue of the vibrational momentum after escape from the well. Orbital AM is generated by an impact parameter (and therefore a b_n) value defined about the same center-of-mass as that for rotational AM, and subject to the same energy constraints. The best match of **j** and **l** will therefore come when the available velocity is apportioned equally between these two modes. The modified A-plot in Figure 4 indicates a peak value of $\Delta N = 8$ or 9 (matching a Δ*l* of the same magnitude) in good agreement with experiment.[23]

Quasiresonant Vibration−Rotation Transfer

We have earlier suggested that OH, like other diatomic hydrides, is likely to fulfill the conditions required for the observation of quasiresonant vibration−rotation transfer (QRT) in some regions of both the $(A)^2\Sigma^+$ and the $(X)^2\Pi$ states. Broadly speaking this requires that the rotational contribution should dominate the overall term energy such that simultaneous near resonance in energy and rotational AM may occur.[9] It is primarily a characteristic of an individual *molecule* therefore and not a strong function of the kinematics or dynamics of a given collision *pair*. In OH, QRT may be more likely to be

observed for ground-state molecules in view of the known rapid predissociation of higher rotational levels of the $(A)^2\Sigma$ excited state. This is particularly effective for $v > 0$.[29] Enhanced VRT pathways in OH were found by Thompson[30] on the basis of classical trajectory calculations and collisional pumping was proposed by Smith and Robinson[31] in their study of the factors influencing laser emission within the $(X)^2\Pi$state.

Much effort has been expended in monitoring OH in different regions of the atmosphere and emission from high N'' levels of $(X)^2\Pi$ has been observed in the night airglow from ground-based experiments by Pendleton et al.[21] and from Space Shuttle measurements under nighttime and quiescent daytime conditions by Smith and co-workers.[22] Both groups remark that the observation of strongly populated high N'' states throws into considerable doubt the assumption of local thermodynamic equilibrium (LTE) in regions of the mesosphere. We have shown above and in ref 8 the practice of fitting the deceptively Boltzmann-like distributions of rotational states from vibration−rotation transfer to obtain a rotational "temperature" to be potentially misleading. The populations adopt a frustrated exponential-like distribution in which low ΔN values are strongly reduced.[8] The assignment of a rotational temperature on the basis of VRT data requires firm corroborative evidence of complete thermalization.

The observations by Smith et al. further highlight problems of description of upper atmospheric rotational state "temperature" since they see strong emission from nonthermalized v, N levels where $N \simeq 26$. Their data is reminiscent of QRT, the existence of which has been experimentally characterized only in the case of high v, j states of $(A)^7Li_2$[10] but which is expected to occur in many other light diatomics.[9] We therefore conclude this survey of a wide range of collisional behavior in the OH radical with an examination of the possibility of QRT in this species. We find that the conditions for QRT exist between numerous N levels of adjacent v states and that the process is likely to occur. We also show that it proceeds with efficiency higher than others we have considered thus far and will consitute a major vibrational relaxation and rotational excitation mechanism (or vice versa) in atmospheric OH. Furthermore, it is a mechanism that will operate at very low translational temperatures.

Spectroscopic and collisional circumstances that will lead to QRT in (X) state OH are illustrated in Figure 6 which shows A- and E-plots for transfer from v, $N = (1, 22)$ and $(2, 31)$ levels of $(X)^2\Pi$ OH to $(0, \Delta N)$ and $(1, \Delta N)$, respectively. These are calculated for the case that N_2 is the principal collision partner. Consider first the E-plot for ($v_i = 1$, $N_i = 22$). The process representing $\Delta N = 0$ requires energy equivalent to 2695 m s^{-1} in order to open this channel. This is more than three times the most probable relative velocity of the collision pair at 300 K and will have very low probability. The situation for $\Delta N = 1$ is little better. Relative velocity in excess of 2350 m s^{-1} is needed to open this channel and limits on maximum value of b_n are very stringent indeed and so this will also be of very low probability. Similarly, all channels other than $\Delta N = 4$ will suffer limitations in the range of b_n that may be accessed. For $\Delta N = 4$ values of b_n are subject to the least restriction and approach the maximum available from the repulsive anisotropy.

Smith et al.[22] report very strong emission from (0, 26) of the (X) state of OH. Other possibilities for $\Delta N = 4$ QRT exist in this region of the OH energy levels and predict $N = 24$, 25, 27, and 28 to be strongly populated. N values close to these are favored for $\Delta N = 4$ QRT from $v = 1$, 2, 3, and 4. Numerous strong bands originating on $v = 0$, 1, and 2 are seen

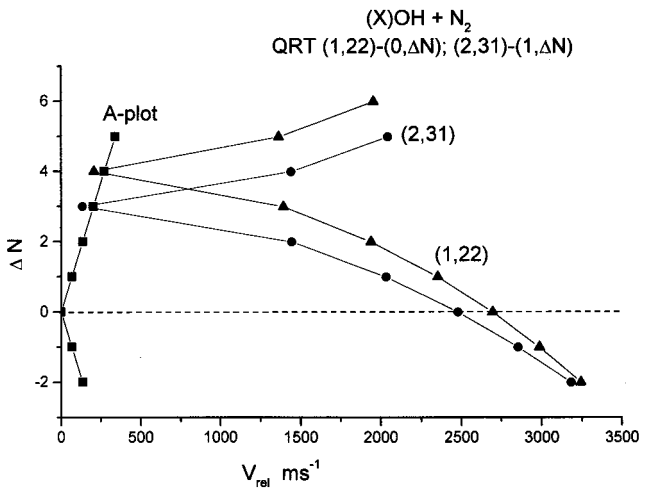

Figure 6. A- and E-plots for the transitions (1, 22) → (0, ΔN) and (2, 31) → (1, ΔN) in $(X)^2\Pi$ OH−N_2 collisions. For the processes $\Delta N = 4$ and $\Delta N = 3$, in these two cases, respectively, the LM → AM mechanism is unconstrained and strong quasiresonant VRT transitions, having narrow ΔN distributions, are predicted.

experimentally[22] in this spectral region corresponding to N values from 30 to 24. The second E-plot in Figure 6 illustrates that the resonances occur at smaller values of ΔN as N increases. We have demonstrated this effect in $^6Li_2$ where $\Delta j = 2$ resonances are predicted for this species at $j_i = 130$.[17] In the case of $(X)^2\Pi$ OH the figure predicts a $\Delta N = 3$ resonance for (2, 31) → (1, 34). It is likely that $\Delta N = 2$ resonances will be seen for higher values of N_i.

The significance of these low ΔN processes is that they have considerably higher cross sections than does $\Delta N = 4$ and these are likely to be major vibrotational transfer mechanisms for this species at high rotational level. It is worth noting that favored collisional routes of this kind exist which permit high vibrational and low rotational states to transfer collisionally to highly rotating, low vibrational state molecules (or the reverse of this process) in pathways that at least preserve, and sometimes enhance the narrowness of the distribution. This clearly occurs in HF[9] and is the secret of that molecule's success as a chemical laser which operates in a multi collision environment at relatively high pressures. Similar behavior is seen in the OH molecule.[31] It is worth reemphasizing the *in*efficiency of rotational relaxation for high values of N_i and so the QRT pathways are likely to dominate when many collisions occur. Under these circumstances, the attainment of thermodynamic equilibrium is slow and the LTE assumption, widely used in atmospheric science, perhaps requires reevaluation, particularly when applied to the regions of the mesosphere where the existence of OH in high N states has been reported.

Conclusions

We have examined the collisional behavior of OH both in its $(A)^2\Sigma^+$ and its $(X)^2\Pi$ state in a wide range of circumstances using a modified form of the AM theory of RT.[1,2,5,8,13] This approach allows an overview of several different forms of collisional interaction which are relevant to the role of the OH radical in atmospheric, interstellar and combustion chemistry. Several new elements emerge from this study some of which relate to a specific form of collision-induced transfer and some are of more general interest. Perhaps the most important of the general observations is that the AM theory provides insight into

the underlying physics of the principal collisional processes and gives rule-of-thumb estimates of the outcome from little more than diagrammatic representations of the kinematics of the interaction.

A further general observation is that the physical *shape* (mass, and size) and spectroscopic properties (rotational and vibrational constants) are the primary determinants of the outcome of a particular collisional interaction. The collision partner can play an important role in determining the state-to-state and overall efficiency of a process through the effect of kinematic constraints. The fine details of the intermolecular potential are irrelevant to this model (except insofar that atomic size provides a sufficiently accurate estimate of the onset of the repulsive wall). Calculations may be carried out with readily available data and these may be made quantitative using hard shape−Monte Carlo methods. Note, however, that we do not attempt to calculate fine structure or λ-doublet branching ratios here.

The process-specific conclusions are as follows. Rotational excitation of OH will be inefficient for all but the lightest collision partners. The fundamental reason for this is the conflicting requirements of energy and AM in this light-heavy diatomic. The LM → AM mechanism is severely constrained by energy conservation such that for N_2 as a collision partner the maximum value of b_n is no more than 0.21 Å. This is to be compared with an expected torque arm of 0.88 Å for this molecule. Possible successful trajectories will therefore be limited to those generating low b_n. The distribution function of ΔN will be exponential-like for rotational excitation although will not be extensive, except for very energetic collisions. Rotational relaxation will suffer more strongly from b_n restriction particularly at low ΔN and thus will be less efficient than excitation (from $N_i = 0$). Energy constraints will be lower for higher values of ΔN, and thus the exponential-like decay of rate constants or probabilities will be shallower than for rotational excitation.

Several distinct VRT processes may be identified each having quite different characteristics. Simultaneous excitation of vibration *and* rotation was the subject of a lengthy discussion by us in a recent publication.[8] The momentum "gap" that must be overcome before rotational AM may be generated in the excited vibrational state plays a crucial role. In OH this is large as a result of the high energy of an OH vibration and the restrictions that energy conservation imposes on b_n at low ΔN will be very severe indeed. As a result the peak of the distribution will be shifted away from $\Delta N = 0$ giving the shape a deceptively Boltzmann-like appearance. It is however best described as a truncated exponential-like distribution in view of the practice of fitting such shapes to a Boltmann distribution and extracting a rotational 'temperature'. This latter process is likely to mislead since the initial rotational distributions from VRT are unlikely to be in thermal equilibrium with their surroundings. Collision velocities needed to open the VRT excitation channel preclude its observation under common laboratory conditions, but the presence of vibrationally excited diatomics, such as N_2 and O_2, and translationally hot atoms indicate increased probability for this process in the upper atmosphere.

More commonly reported is VRT data involving simultaneous vibrational relaxation with rotational excitation and in this case the kinematic plots reveal a more complex interplay. Vibrational relaxation requires that the vibrational momentum and energy be disposed of into OH rotation but this is limited by energetic considerations and the high rotational constant of this molecule. When an atom is the collision partner, conservation of energy and total angular momentum become incompatible and the relaxation is inefficient. A diatomic partner however can provide a very convenient sink for a large fraction of the vibrational momentum and VRT becomes much more probable. The shape of the modified A-plot and the revised maximum b_n values for each channel readily explains the "bimodal" shapes of the VRT distributions. The problem of balancing energy and total AM factors is crucial to the photodissociation of the OH−Ar van der Waals complex on excitation of $v = 1$ in OH. When these are matched, the velocity−AM plot is an accurate predictor of N state distribution and this suggests such diagrams may provide more general insights into the dissociation of such species.

Finally, we predict that quasiresonant VRT is likely to occur in high lying rotational levels of ground and excited OH, though may not be observable in $(A)^2\Sigma$ because of predissociation. $\Delta N = 4$ resonances are expected around $N = 26$ of the lower v levels and $\Delta N = 3$ processes in the region of $N = 34$. They have *much* higher probability than rotational relaxation for these levels. Strong OH emission from $N = 26$, likely to result from QRT, has already been reported in Space Shuttle based observations of the night airglow.[21]

References and Notes

(1) McCaffery, A. J.; AlWahabi, Z.T.; Osborne, M. A.; Williams, C. J. *J. Chem. Phys.* **1993**, *98*, 4586. AlWahabi, Z. T.; McCaffery, A. J. *Phys. Rev. A* **1991**, *43*, 611.

(2) Osborne, M. A.; McCaffery, A. J. *J. Chem. Phys.* **1994**, *101*, 5604.

(3) Marks, A.J. *J. Chem. Soc., Faraday. Trans.* **1994**, *90*, 2857.

(4) Clare, S.; Marks, A. J.: McCaffery, A. J. *J. Phys. Chem. A* **2000**, *104*, 7181.

(5) Clare, S.; Marks, A. J.; McCaffery, A. J. *J. Chem. Phys.* **1999**, *111*, 9287.

(6) Kreutz, T. G.; Flynn, G. W. *J. Chem. Phys.* **1990**, *93*, 452.

(7) R.Marsh and A. J.McCaffery, *Chem. Phys. Lett.* **2001**. To be published.

(8) McCaffery, A. J.; Marsh, R. J. *J. Phys. Chem. A* **2000**, *104*, 10442.

(9) Clare, S.; McCaffery, A. J. *J. Phys. B* **2000**, *33*, 1121.

(10) Stewart, B.; Magill, P. D.; Scott, T. P.; Derouard, J.; Pritchard, D. E. *Phys. Rev. Lett.* **1988**, *60*, 282.

(11) Thompson, D. L. *J. Phys. Chem.* **1982**, *86*, 2538.

(12) Downey, G.D.; Robinson, G. W.; Smith, J. H. *J. Chem. Phys.* **1977**, *66*, 1685.

(13) McCaffery, A. J. *J. Chem. Phys.* **1999**, *111*, 7697.

(14) Besley, N.A.; McCaffery, A.J.; Osborne, M. A.; Rawi, Z. *J. Phys. B* **1998**, *31*, 4267.

(15) Brunner, T. A.; Pritchard, D. E. *Adv. Chem. Phys.* **1982**, *50*, 589.

(16) Li, J.; Bahns, J. T.; Stwalley, W. C. *J. Chem. Phys.* **2000**, *112*, 6255.

(17) McCaffery, A. J. *J. Chem. Phys.* **2000**, *113*, 10941.

(18) Lengel, R. K.; Crosley, D. R. *J. Chem. Phys.* **1977**, *67*, 2085.

(19) Lengel, R. K.; Crosley, D.R. *J. Chem. Phys.* **1977**, *68*, 5309. Crosley, D. R. *J. Phys. Chem.***1989**, *93*, 6273. Williams, L. R.; Crosley, D. R. *J. Chem. Phys.* **1996**, *104*, 6507.

(20) Jörg, A.; Meier, U.; Kohse-Höinghaus, K. *J. Chem. Phys.* **1990**, *93*, 6453.

(21) Pendleton, W.; Espy, P.; Baker, D.; Steed, A; Fetrow, M.; Henrikson, K. *J. Geophys. Res.* **1989**, *94*, 505.

(22) Smith, D.R.; Blumberg, W.A. M.; Nadile, R. M.; Lipson, S.J.; Huppi, E.R.; Wheeler, N. B.; Dodd, J. A. *Geophys. Res. Lett.* **1992**, *19*, 593.

(23) Berry, M.T.; Brustein, M.R.; Lester, M. I. *J. Chem. Phys.* **1990**, *92*, 6469. Lester, M.L.; Choi, S.E.; Giancarlo, L.C.; Randall, R.W. *J. Chem. Soc., Faraday Discuss.* **1994**, *97*, 365.

(24) Bosanac, S. D.; Buck, U. *Chem. Phys. Lett.* **1981**, *81*, 315.

(25) Degli Esposti, A.; Werner, H. J. *J. Chem. Phys.* **1990**, *93*, 3351.

(26) DePristo, A. E.; Augustine, S. D.; Ramaswami, R.; Rabitz, H. *J. Chem. Phys.* **1979**, *71*, 850. Brunner, T. A.; Driver, R. D.; Smith, N.; Pritchard, D. E. *J. Chem. Phys.* **1979**, *70*, 4155.

(27) Korsch, H. J.; Ernesti, R. *J. Phys. B* **1992**, *25*, 3565.

(28) Yardley, J. T. *Introduction to Molecular Energy Transfer*; Academic Press: New York, 1982

(29) Sutherland, R. A.; Anderson, R. A. *J. Chem. Phys.* **1973**, *58*, 1226.

(30) Thompson, D. L. *J. Phys. Chem.* **1982**, *86*, 2538.

(31) Smith, J. H.; Robinson, D. W. *J. Chem. Phys.* **1978**, *68*, 5474.